Review

Atmospheric Plasma Deposition of Coatings Using a Capacitive Discharge Source**

By *Maryam Moravej* and *Robert F. Hicks**

In this paper, a review is provided of the plasma-enhanced (PE)CVD of thin films using an atmospheric-pressure (AP) capacitive discharge source. This source is unique in that the organometallic precursors are fed downstream of the plasma, where reactions occur exclusively between neutral molecules, radicals, and the substrate surface. As a result, the properties of the films differ from those obtained in low-pressure (<1 torr) gas discharges. For example, glass may be deposited on plastic with no carbon contamination and less than 15 mol-% hydroxyl groups, yielding material with good scratch protection. Silicon nitride and amorphous hydrogenated silicon films have also been prepared by AP-PECVD. These material processes further illustrate the unique attributes of this new deposition technology.

Keywords: Atmospheric-pressure plasma, Deposition, PECVD

© WILEY-VCH

1. Introduction

PECVD is widely used in the microelectronics, automotive, and aerospace industries for the deposition of thin films and hard coatings.[1–6] Traditional PECVD systems operate under reduced pressures, between 1.0 mtorr and 5000 mtorr.[1,7–9] Examples of low-pressure plasmas are capacitive discharges, inductively coupled plasmas (ICP), and electron cyclotron resonance (ECR) sources.[1–5] However, there is interest in using AP plasmas for materials processing, since they may be adapted to large substrates that are manufactured in a continuous fashion.

AP discharges fall into two main categories: thermal and non-equilibrium systems. Thermal plasmas, such as ICP torches, exhibit ion, electron, and neutral gas temperatures that are approximately equal to each other and range from 3000 K to 20000 K.[10–16] These devices are used to produce a variety of hard coatings, such as diamond-like carbon films.[17–19] Non-equilibrium plasmas exhibit neutral and ion temperatures that are two to three orders of magnitude lower than their electron temperature. The ion and neutral temperatures range from 273 to 1000 K, whereas the electron temperature is much higher, between 10^4 and 10^5 K, or 1 to 10 eV.[20] In these plasmas, the energetic electrons dissociate the gas molecules to form reactive radical and ionic species that are well-suited to the deposition of thin films.

[*] Prof. R. F. Hicks, Dr. M. Moravej
Department of Chemical Engineering, University of California, Los Angeles,
5531 Boelter Hall, Los Angeles, CA 90095 (USA)
E-mail: rhicks@ucla.edu

[**] This work was supported by a grant from Motorola, Inc.

It is challenging to generate non-equilibrium plasmas under atmospheric pressure. Higher voltages are required for gas breakdown under this pressure, and arcing between the electrodes can occur. Although the focus of this paper will be on radio frequency (RF) discharges, many other types of low-temperature plasmas have been developed that use either DC, low frequency AC, or microwave power. These include coronas,[21,22] dielectric barrier discharges (DBD),[23–29] and microhollow cathode discharges (MHCD).[30–32]

There are many reports of RF atmospheric-pressure discharges that utilize a coaxial electrode design.[33–40] In these sources, one of the electrodes is a metallic rod that is enclosed in another cylindrical electrode. Either one of the electrodes can be powered. Gas flows between the electrodes, where the plasma is ignited and sustained. In some of these devices, the anode is covered with an insulator such as alumina or quartz to help stabilize the discharge.[33,36,38,40,41] Koinuma and coworkers have reported a coaxial design where the cathode is a thin rod (which is referred to as a needle) the anode is a metallic cylinder, and an alumina tube is placed between the two electrodes.[40,41] This design is referred to as a cold plasma torch because the temperature is 450 °C. This source has been used to deposit silicon dioxide using argon and tetramethoxysilane at rates of about 600 nm min^{-1}.[40] Collins and coworkers reported on a RF atmospheric pressure plasma with a gas temperature of about 480 °C.[42] This plasma source is similar to a corona because the cathode has a pointed tip to create a region of high electric field to facilitate the ignition process. However, to avoid the streamer-like discharge of a corona, helium is added to the gas to create a diffuse glow.

Another type of RF plasma uses planar electrodes that are parallel to each other.[25,26,43,44] In these sources, an in-

 © 2005 WILEY-VCH Verlag GmbH & Co. KGaA, Weinheim

sulator is placed on one or both of the electrodes to prevent arcing, and a rare gas is added to create a diffuse glow. These designs are similar to DBDs except that RF power is employed instead of low frequencies between 20 Hz and 20 kHz. Most of the PECVD studies reported with DBDs do not use RF power and are direct, where the substrate is placed in contact with the plasma,[45–50] while only one remote deposition system has been reported.[51] In this latter study, SiO_2 films were grown on silicon substrates using the filamentary mode with a gas mixture of Ar and O_2. Hexamethyldisiloxane (HMDSO) was used as the silicon precursor. Growth rates of 12 nm min^{-1}, at a substrate temperature of 500 °C, were reported.[51]

MHCDs are DC glow discharges sustained between two parallel metal electrodes with a center opening of diameter 0.1 mm in either the cathode, or the cathode and the anode.[30,31] The electrodes are separated by a gap of 0.2–0.4 mm, which is often filled with a dielectric material.[52–55] The MHCD is normally supplied with DC power, and operated in Ar, Xe, and air.[30,31,52] Barankova and coworkers have reported the operation of a MHCD with RF power.[32,56] Hollow cathode discharges are mostly used as light sources, and deposition with these devices has been limited. [30,54,57] Guo et al.[58] have deposited amorphous carbon films under atmospheric pressure using a RF microhollow cathode source fed with 1.0 vol.-% hexamethyldisiloxane and helium, and operated at 13.56 MHz and 440 W cm^{-3}.

Capacitive discharges stabilized with inert gas have been the focus of research in our laboratory over the past five years.[59–73] These devices are well-suited to the AP-PECVD of thin films. In this paper, we will describe the physics and chemistry of these plasmas, as well as their use for the deposition of silicon dioxide, silicon nitride, and amorphous hydrogenated silicon films. It will be shown that these discharges access a unique process window that can be beneficial to the material properties.

2. Plasma Source Design

The AP-PECVD apparatus developed in our laboratory is shown in Figure 1. The plasma source consists of two

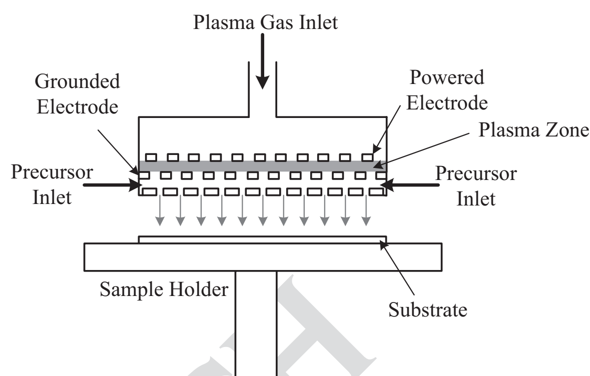

Fig. 1. Schematic of the AP-PECVD apparatus.

closely spaced, perforated metal electrodes, the upper electrode being coupled to RF power at 13.56 MHz, while the lower electrode is grounded. Helium or argon, together with <3.0 vol.-% oxygen, nitrogen, or hydrogen are passed through the electrodes and excited to make a weakly ionized plasma. An inlet distributor is incorporated into the grounded electrode, so that the organometallic precursor may be introduced into the flow of gaseous reactive species emerging from the plasma. Downstream addition ensures that the deposition chemistry is restricted to reactions between neutral species. Under atmospheric pressure, the charged particle density decays very rapidly in the afterglow, whereas the atoms and radicals generated by the plasma are relatively long lived.[60,65,73] The chemical precursor reacts with the atoms and radicals, and then impinges on the substrate and deposits the thin film.

3. Discharge Physics

Current and voltage waveforms for a helium discharge operated under 760 torr and at 20 W cm^{-3} are shown in Figure 2. The maximum operating voltage and current are approximately 280 V and 1.0 A, and both parameters exhibit sinusoidal curves. The waveforms indicate a capacitive discharge because the phase angle between the current and the voltage is approximately 86°. The 4° shift in phase angle

Robert F. Hicks is a Professor of Chemical Engineering at the University of California, Los Angeles, and Chief Executive Officer of Surfx Technologies LLC in Culver City, California. He received his B. S. and Ph.D. degrees in chemical engineering from the University of Delaware in 1977 and the University of California, Berkeley, in 1984. He has been a faculty member at UCLA since 1985. His research interests are in atmospheric pressure plasmas and materials processing. Robert has authored over 130 scientific papers and is an inventor on 6 U. S. patents. He is a member of the AVS, TMS and AIChE. In 2001, he was elected Fellow of the American Vacuum Society. In 1999, he received an R&D 100 Award for co-invention of the atmospheric pressure plasma jet.

© WILEY-VCH

 © 2005 WILEY-VCH Verlag GmbH & Co. KGaA, Weinheim

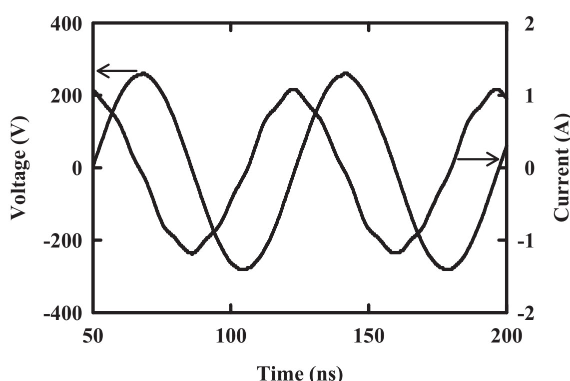

Fig. 2. Current and voltage waveforms for the RF discharge with helium under 760 torr and at 20 W cm^{-3}.

is due to the resistive component arising from the ionized gas.[74]

The capacitive discharge source exhibits physics that are similar to low-pressure DC discharges. Shown in Figure 3 is a current-voltage plot for helium under atmospheric pressure. Prior to gas breakdown, there is a Townsend dark re-

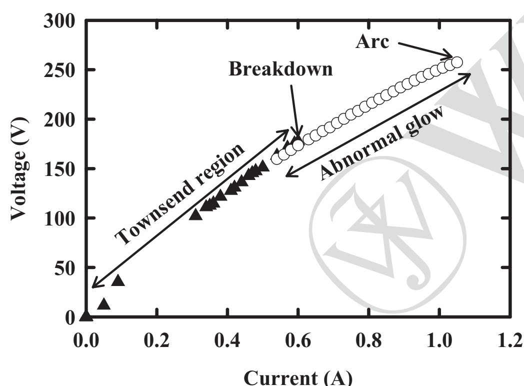

Fig. 3. Current-voltage plot for helium under 760 torr.

gion where the voltage increases linearly with the current. Breakdown occurs at 180 V and 0.6 A, followed by an immediate decrease to 150 V and 0.5 A. Beyond this point, the discharge operates in the abnormal glow regime, where the voltage rises with the current. At approximately 260 V and 1.1 A, the plasma transforms into an arc, and is turned off. Using these current-voltage curves, the plasma density and electron temperature for the helium discharge have been calculated. At a power density of 12 W cm^{-3}, which corresponds to operation at 170 V and 0.6 A on the abnormal glow curve, the electron density and temperature are determined to be 9.3×10^{11} cm^{-3} and 2.4 eV, respectively.

4. Discharge Chemistry

The afterglow chemistry of the atmospheric pressure plasma has been studied using spectroscopic techniques.[65,67,71] The apparatus used in these experiments consists of two parallel metal plates separated by a gap of 1.6 mm. Helium, and oxygen or nitrogen, flow through these electrodes and are ionized with RF power at 13.56 MHz. The powered electrode area is 10.2×5.5 cm^2 in the case of He and O_2, and 10.2×7.9 cm^2 in the case of He and N_2. The sides of the device are fitted with quartz windows to allow for spectroscopic measurements of the gas.[65,67,71]

The species that have been investigated in the helium and oxygen plasma are ground-state oxygen atoms, $O(^3P)$; singlet-delta metastable oxygen, $O_2(^1\Delta_g)$; singlet-sigma metastable oxygen, $O_2(^1\Sigma_g^+)$; and ozone, O_3.[71] The ozone concentration has been determined using ultraviolet absorption spectroscopy. The $O_2(^1\Delta_g)$ and $O_2(^1\Sigma_g^+)$ densities have been measured using optical emission and infrared spectroscopies, respectively. These results have been combined in a numerical model to calculate the O atom density in the afterglow of the discharge. At a maximum power density of 30.5 W cm^{-3}, a gas temperature of 100 ± 40 °C, and an O_2 feed of 1.5×10^{17} cm^{-3}, the plasma generates 1.0×10^{16} cm^{-3} of $O(^3P)$ and $O_2(^1\Delta_g)$, 2.0×10^{15} cm^{-3} of $O_2(^1\Sigma_g^+)$, and 1.0×10^{15} cm^{-3} of O_3.[71] It has been found that the etching rate of polyimide correlates with the concentration of oxygen atoms in the afterglow, indicating that these species may be involved in this process.[60,71]

The active species found in the afterglow of an ambient pressure helium and nitrogen plasma are nitrogen atoms, $N(^4S)$, and metastable nitrogen molecules, $N_2(A^3\Sigma_u)$, $N_2(B^3\Pi_g)$, and $N_2(C^3\Pi_u)$. The concentrations of $N_2(B^3\Pi_g)$ and $N_2(C^3\Pi_u)$ have been found using optical emission, while the density of $N_2(A^3\Sigma_u)$ has been determined by optical absorption.[64] At 15.5 W cm^{-3}, 10 torr N_2, 750 torr He, and 50 °C, the plasma produces 2.1×10^{13} cm^{-3} $N_2(A^3\Sigma_u)$, 1.2×10^{12} cm^{-3} $N_2(B^3\Pi_g)$, and 3.2×10^9 cm^{-3} $N_2(C^3\Pi_u)$. To determine the concentration of the ground-state nitrogen atoms, three methods have been employed; nitric oxide titration, absolute intensity measurement of the $N_2(B^3\Pi_g)$ emission, and temporal decay of the $N_2(B^3\Pi_g)$ emission.[64] Based on these measurements, the atmospheric pressure plasma produces a high density of nitrogen atoms, exceeding 4.0×10^{15} cm^{-3} at the edge of the discharge for 10 torr N_2 in 750 torr He at 50 °C and 15.5 W cm^{-3}.[65,67]

5. Processing with the RF Inert Gas Plasma

5.1. PECVD of Silicon Dioxide

Silicon dioxide films have been deposited using the plasma source depicted in Figure 1. The discharge is operated with a mixture of helium and 2 vol.-% oxygen, and an organometallic precursor is added downstream where it reacts with the species exiting the plasma. Note that this is a remote PECVD process, where the substrate is not in contact with the plasma, so there is no ion bombardment of

 © 2005 WILEY-VCH Verlag GmbH & Co. KGaA, Weinheim

the surface. The films have been deposited on both silicon substrates and plastic coupons at temperatures below 100 °C.[72]

The precursors examined in this study were hexamethyldisilazane (HMDSN), hexamethyldisiloxane (HMDSO), tetramethyldisiloxane (TMDSO), tetramethylcyclotetrasiloxane (TMCTS), and tetraethoxysilane (TEOS). Shown in Figure 4 is a plot of the deposition rate as a function of the precursor partial pressure for all these chemicals.[43] The growth rates observed with TMCTS, TEOS, and HMDSN

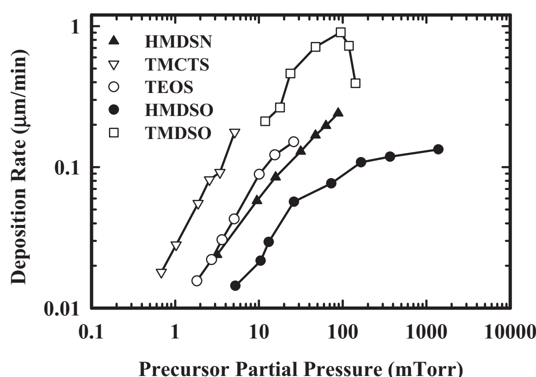

Fig. 4. Silicate glass deposition rate as a function of the precursor type and partial pressure.

are proportional to the precursor partial pressure, and increase from about 15 nm min^{-1} to 200 nm min^{-1}. Similar results have been reported for low pressure PECVD processes with TEOS.[75,76]

The deposition rate with HMDSO exhibits similar values; however, it gradually levels off beyond 200 mtorr. In contrast to these results, the growth rate obtained with TMDSO increases from 200 nm min^{-1} to 1000 nm min^{-1} as the partial pressure rises from 10 mtorr to 100 mtorr. Above 100 mtorr, the deposition rate falls with the TMDSO partial pressure.[72] It can be seen that the deposition rate is strongly dependent on the precursor used.

The following maximum rates have been reported in the literature for low pressure PECVD: 1000 nm min^{-1} using HMDSO and TMCTS,[77] 10000 nm min^{-1} with TEOS,[78] 400 nm min^{-1} with HMDSN,[79] and 1300 nm min^{-1} with TMDSO.[80] Most of these films were grown using either ECR or capacitively coupled plasmas operating under pressures below 100 mtorr, with the precursor molecules fed directly into the discharge. Since the precursor is fed into the plasma, it is subject to dissociation by both neutral chemistry and electron impact.[1] However, only neutral chemistry occurs in the atmospheric plasma deposition process. This would explain why the low-pressure plasma processes generally yield higher deposition rates than those observed here.

The choice of organosilane precursor also affects the film properties. Shown in Figure 5 are infrared spectra of films grown with HMDSN and TMDSO at their maximum de-

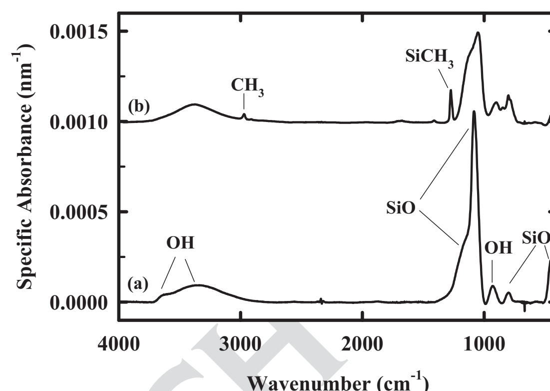

Fig. 5. Infrared spectra of SiO_2 deposited with a) HMDSN and b) TMDSO.

position rates of 240 nm min^{-1} and 910 nm min^{-1}, respectively. The peaks at 1075 cm^{-1}, 800 cm^{-1}, and 450 cm^{-1} are due to the asymmetric stretching, bending, and rocking modes of siloxane bridges.[64,81–83] The broad shoulder at ~1150 cm^{-1} is also due to the stretching modes of the siloxane bridges.[64,83] The peak at 930 cm^{-1} is due to O–H deformations, while the broad band and shoulder at 3400 cm^{-1} and 3650 cm^{-1} are due to O–H stretching vibrations of hydrogen-bonded and isolated hydroxyl groups.[64,81] In the film grown with TMDSO, C–H bending and stretching modes are observed at 1275 cm^{-1} and 2900 cm^{-1}. These modes are due to the presence of methyl groups attached to silicon.[84,85] The infrared spectra of the SiO_2 film deposited with TMDSO shows a significantly different distribution of bands than the spectra of the film deposited with HMDSN. In particular, the siloxane peaks at 1075 cm^{-1}, 800 cm^{-1}, and 450 cm^{-1} are greatly reduced in intensity, while the shoulder at 1150 cm^{-1} has become broader and more intense. These changes are attributed to increased film porosity.[84–87] Based on quantitative analysis of the infrared spectra, the glass grown with TMDSO contains 20 mol-% OH, whereas the glass deposited with HMDSN, contains 13 mol-% OH and there is no carbon contamination.

Figure 6 shows optical microscope images of 1500 nm thick glass films grown on plastic. These samples have been scratched with steel wool to test their abrasion resistance. Figures 6a and 6b illustrate films grown with TMDSO at 910 nm min^{-1} and HMDSN at 240 nm min^{-1}. It can be seen that the film deposited with HMDSN exhibits only two scratches per mm, while the film deposited with TMDSO has eleven scratches per mm. Comparison of this data with the infrared spectra of Figure 5 indicates that the poor abrasion resistance observed in the latter case is most likely due to higher porosity and to the incorporation of methyl groups into the glass matrix.[72] These results clearly indicate that the organosilicon precursor used in the PECVD process strongly influences the chemical and mechanical properties of the glass films.

© WILEY-VCH

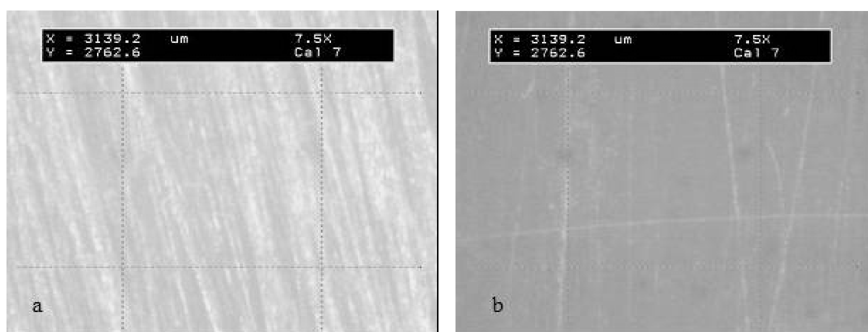

Fig. 6. Microscope images of scratched glass films prepared from a) TMDSO and b) HMDSN.

5.2. PECVD of Silicon Nitride

Silicon nitride has been deposited on silicon wafers under atmospheric pressure and at temperatures between 100 °C and 500 °C, using the apparatus shown in Figure 1.[66] Helium and nitrogen were fed to the plasma, while the silane was added downstream. A maximum growth rate of 130 ± 13 nm min^{-1} was observed.[66] This rate is two to three times higher than those recorded in low-pressure, remote PECVD systems. The effect on the growth rate of the N_2 and SiH_4 partial pressures is shown in Figure 7.[66] The rate increases with the nitrogen partial pressure, exhibiting a reaction order in N_2 of 0.5. The maximum pressure of nitrogen that can be fed to the plasma is 19 torr. Above this value, the plasma converts to an arc. The deposition rate increases with SiH_4 partial pressure as well, but the reaction order is only 0.1 at partial pressures of SiH_4 between 0.07 and 2.0 torr. Below 0.07 torr, the rate falls off quickly. In low-pressure processes, the growth rate also increases with increasing SiH_4 and N_2 partial pressures.[88–90] The growth rate is invariant with respect to temperature and substrate rotational speed. The deposition rate also decreases sharply with distance from the plasma. There have been several studies of remote PECVD systems with ECR plasmas under low pressures that yield growth rates in the range 50–60 nm min^{-1}.[88–93] By comparison, our AP plasma deposits silicon nitride films of the same quality at double the rate.

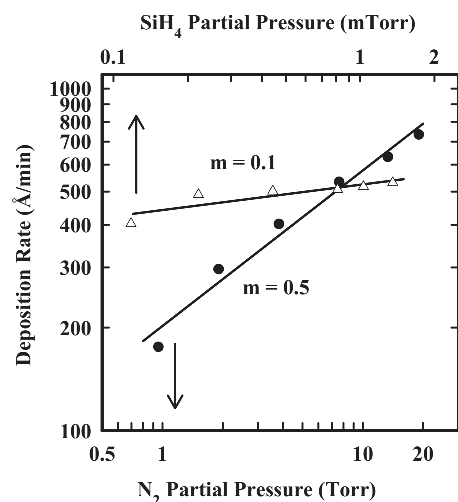

Fig. 7. Deposition rate of Si_3N_4 as a function of the N_2 and SiH_4 partial pressures.

Shown in Figure 8 is a plot of the hydrogen content and its bond type in the silicon nitride as a function of the ratio of the N_2 to SiH_4 pressure in the afterglow.[66] At low ratios, the total hydrogen content is roughly 13 at.-% distributed equally between the Si and N. As the N_2 partial pressure increases, more hydrogen atoms attach to nitrogen, while the number of Si–H bonds gradually decreases. At the maximum N_2:SiH_4 ratio of 84, the total hydrogen content is 20 at.-%, with 85 % of the bonds due to N–H.[66] While the total hydrogen content of the silicon

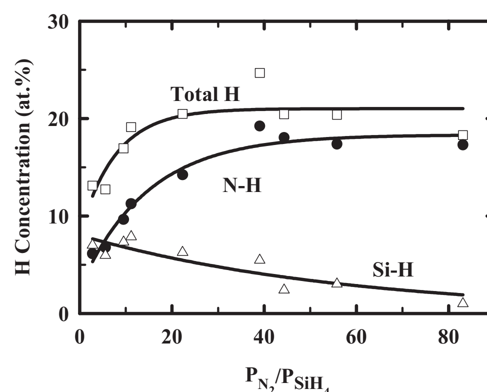

Fig. 8. Hydrogen content of the Si_3N_4 films as a function of the ratio of the N_2 to SiH_4 partial pressures.

nitride deposited under atmospheric pressure is similar to that under low pressure, the bond arrangement is different. In low-pressure N_2/SiH_4 plasmas, the hydrogen bonds to silicon and, in most cases, there is no detectable N–H.[82,94,95] By contrast, the N–H bonds dominate when ammonia is substituted for N_2 in the gas feed.[82,92,95]

It has been shown that the conformality of silicon nitride films correlates with the hydrogen bond type. When NH_3 and SiH_4 are used in low-pressure plasmas, the conformality of films on patterned silicon wafers is >60 %, whereas when N_2 and SiH_4 are used, it is only 10 %.[96] The conformality is defined as the ratio of the film thickness at the bottom of a feature to that at the top. Our group has found that silicon nitride films grown by remote PECVD under atmospheric pressure with N_2 and SiH_4 exhibit a high degree of conformality and, as discussed above, show a predominance of N–H bonding. For example, a film was deposited on a patterned gallium arsenide wafer under a

 © 2005 WILEY-VCH Verlag GmbH & Co. KGaA, Weinheim

pressure of 760 torr, 7.6 torr N_2, 0.3 torr SiH_4, 42 W cm^{-3}, 300 °C, and an electrode-to-substrate spacing of 7.6 mm. A scanning electron microscope (SEM) image of this film is presented in Figure 9. It can be seen that the film evenly coats the feature so that the thickness on the lower terrace, upper terrace, and side wall equals 200 nm, 220 nm, and 240 nm, respectively, with a standard deviation of 9.0 %. The conformality of this film equals 90 %.

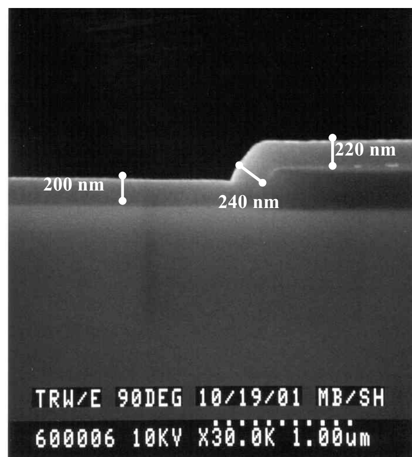

Fig. 9. SEM image of Si_3N_4 deposited on a patterned GaAs wafer.

5.3. PECVD of Amorphous Hydrogenated Silicon

Amorphous hydrogenated silicon (α-Si:H) has been deposited under atmospheric pressure and at a low temperature using a hydrogen and helium plasma, and with a downstream addition of silane.[68] A maximum deposition rate of 12 ± 1 nm min^{-1} is recorded at 450 °C, 6.3 torr H_2, 0.3 torr SiH_4, 778 torr He, 32.8 W cm^{-3}, and an electrode-to-substrate spacing of 6.0 mm. The deposition rate increases rapidly with the silane and hydrogen partial pressures, up to 0.1 torr and 7.0 torr, respectively, then remains constant thereafter. By contrast, the deposition rate decreases exponentially as the electrode-to-substrate distance is increased from 5.0 mm to 10.5 mm.[68] Other groups have reported deposition rates ranging from 0.5 nm min^{-1} to 3.5 nm min^{-1} using an ICP source operating under 0.2 torr and with a 200 °C substrate temperature.[97,98] These results may be compared to the present study, where a deposition rate of 6.5 nm min^{-1} was recorded under atmospheric pressure and at 200 °C. It should be noted that rates as high as 600 nm min^{-1} have been achieved with an expanding thermal plasma (cascaded arc) which, although a remote system, has a high density of ionic and thermally activated species that can be involved in the gas phase reactions.[99]

Shown in Figure 10 is the dependence of the hydrogen content on the H_2 pressure. The growth conditions are 300 °C, 0.3 torr SiH_4, and an electrode-to-substrate distance of 6.0 mm. The total hydrogen concentration de-

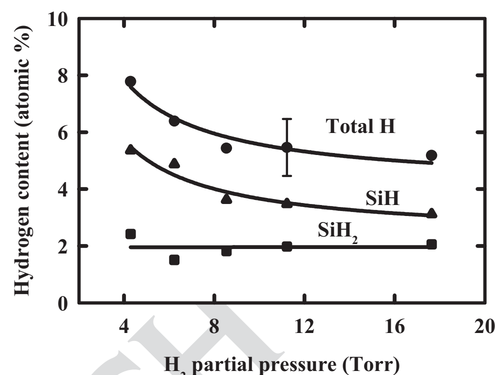

Fig. 10. The dependence of the hydrogen content in the α-Si:H film on the H_2 partial pressure in the atmospheric plasma.

creases from 8.0 at.-% to 5.0 ±1.0 at.-% as the H_2 pressure rises from 4.3 torr to 17.6 torr. The silicon monohydride species follows a similar trend, decreasing in concentration from 5.5 at.-% to 3.0 at.-%. By contrast, the silicon dihydride species stays constant at 2.0 at.-%. At the higher H_2 pressures, approximately three quarters of the total hydrogen is in the monohydride form.[68] These results may be compared to remote low-pressure PECVD, where the total hydrogen content ranges from 7.0 at.-% to 15.0 at.-%.[99–106]

A numerical model has been developed to investigate the dependence of the SiH_3 concentration in the afterglow on the SiH_4 pressure in the feed. These results are illustrated in Figure 11 for the SiH_3 concentration calculated 6 mm below the bottom electrode. It can be seen that the silyl radical density quickly rises to about 1.5×10^{13} cm^{-3} under 0.1 torr SiH_4,

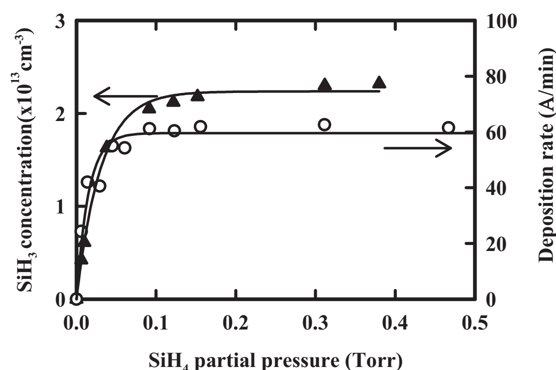

Fig. 11. The dependence of the predicted SiH_3 concentration and the observed deposition rate on the SiH_4 partial pressure in the atmospheric plasma.

and thereafter remains constant as the silane pressure increases further. The knee in the curve corresponds to the "titration point," where the concentration of SiH_4 equals that of the H atoms. The silane pressure is 0.02 torr at the knee, yielding a species density of 2.1×10^{15} cm^{-3}. This value is in good agreement with the H atom concentration estimated from the numerical model, which equals 2.6×10^{15} cm^{-3}.[68]

© WILEY-VCH

In Figure 11, the observed dependence of the deposition rate on the silane pressure is shown so that it may be compared directly to the simulations. The trend in the deposition rate closely follows that exhibited by the SiH_3 concentration. Based on these results, it may be surmised that H atoms and silyl radicals are important reactive intermediates in the PECVD process, and that the concentration of H atoms produced by the helium-stabilized, atmospheric-pressure plasma is in the range $2.0 \pm 1.0 \times 10^{15}$ cm^{-3}.[68] The low hydrogen content in the films deposited under atmospheric pressure is most likely related to the higher concentration of radicals produced in the atmospheric-pressure discharge, e.g., 10^{15} cm^{-3} of H atoms, and 10^{13} cm^{-3} of SiH_3.[107,108] The increased radical pool should lead to higher rates of hydrogen abstraction from the film surface.[109–111]

6. Summary and Prognosis

Low-temperature, atmospheric-pressure plasmas are promising tools for the deposition of thin films. The advantages of these discharges are that they can coat thermally-sensitive materials, such as plastics and polymers, and are well suited to continuous, in line processing. Moreover, the size and shape of the substrate to be processed is not restricted by the dimensions of the plasma source. We have described a new plasma source for the remote PECVD of thin films, and demonstrated its application to silicon dioxide, silicon nitride, and amorphous hydrogenated silicon deposition. It has been found that remote PECVD under atmospheric pressure creates a new process window with alternative reaction chemistry that leads to improved material properties. We expect that further discoveries will be made as atmospheric plasma deposition is explored for other applications.

Received: September 10, 2004
Final version: March 11, 2005

[1] M. A. Lieberman, A. J. Lichtenberg, *Principles of Plasma Discharges and Materials Processing*, Wiley Interscience, New York **1994**.
[2] W. Luft, Y. S. Tsuo, *Hydrogenated Amorphous Silicon Alloy Deposition Processes*, Marcel Dekker, Inc., New York **1993**.
[3] G. Bruno, P. Capezzuto, A. Madan, *Plasma Deposition of Amorphous Silicon-Based Materials*, Academic Press, Boston, MA **1995**.
[4] M. Konuma, *Film Deposition by Plasma Techniques*, Springer-Verlag, Berlin, **1992**.
[5] R. A. Street, *Technology and Applications of Amorphous Silicon*, Springer-Verlag, Berlin **2000**.
[6] F. F. Chen, *Introduction to Plasma Physics and Controlled Fusion*: *Vol. 1 Plasma Physics*, Plenum Press, New York **1984**.
[7] J. D. Chapple-Sokol, W. A. Pliskin, R. A. Conti, *J. Electrochem. Soc.* **1991**, *138*, 3723.
[8] S. Sahli, S. Rebiai, P. Raynaud, Y. Segui, A. Zenasni, S. Mouissat, *Plasmas Polym.* **2002**, *7*, 327.
[9] D. E. Kotecki, J. D. Chapple-Sokol, *J. Appl. Phys.* **1995**, *77*, 1284.
[10] P. Fauchais, A. Vardelle, *IEEE Trans. Plasma Sci.* **1997**, *25*, 1258.
[11] R. W. Smith, D. Wei, D. Apelian, *Plasma Chem. Plasma Process.* **1989**, *9*, 135S.
[12] S. Ramakrishnan, M. W. Rogozinski, *J. Phys D*: *Appl.Phys.* **1997**, *30*, 636.
[13] S. Ramakrishnan, M. Gershenzon, F. Polivka, T. N. Kearney, M. W. Rogozinski, *IEEE Trans. Plasma Sci.* **1997**, *25*, 937.
[14] M. H. Gordon, C. H. Kruger, *Phys. Fluids B* **1993**, *5*, 1014.
[15] M. Abdur Razzak, K. Kondo, Y. Uesugi, N. Ohno, S. Takamura, *J. Appl. Phys.* **2004**, *95*, 427.
[16] H. Huang, X. Yao, *Ceram. Int.* **2004**, *30*, 1535.
[17] M. Zhao, T. G. Owano, C. H. Kruger, *Diamond Relat. Mater.* **2001**, *10*, 1565.
[18] Y. Mori, K. Yoshii, H. Kakiuchi, K. Yasutake, *Rev. Sci. Instrum.* **2000**, *71*, 3173.
[19] S. K. Baidwin, Jr., T. G. Owano, M. Zhao, C. H. Kruger, *Diamond Relat. Mater.* **1997**, *6*, 202.
[20] H. E. Wagner, R. Brandenburg, K. V. Kozlov, A. Sonnenfeld, P. Michel, J. F. Behnke, *Vacuum*, **2003**, *71*, 417.
[21] M. Goldman, N. Goldman, in *Gaseous Electronics*: *Vol. 1*, (Eds: M. N. Hirsh, H. J. Oakam), Academic, New York **1978**.
[22] J. S. Chang, P. A. Lawless, T. Yamamoto, *IEEE Trans. Plasma Sci.* **1991**, *19*, 1152.
[23] B. Eliasson, U. Kogelschatz, *IEEE Trans. Plasma Sci.* **1991**, *19*, 1063.
[24] V. I. Gibalov, G. J. Pietsch, *J. Phys. D*: *Appl. Phys.* **2000**, *33*, 2618.
[25] S. Kanazawa, M. Kogoma, T. Moriwaki, S. J. Okazaki, *J. Phys. D*: *Appl. Phys.* **1988**, *21*, 836.
[26] T. Yokoyama, M. Kogoma, T. Moriwaki, S. J. Okazaki, *J. Phys. D*: *Appl. Phys.* **1990**, *23*, 1125.
[27] D. Trunec, A. Brablec, F. Stastny, *Contrib. Plasma Phys.* **1998**, *38*, 435.
[28] F. Massines, A. Rabehi, P. Descomps, R. B. Gadri, P. Segur, C. Mayoux, *J. Appl. Phys.* **1998**, *83*, 2950.
[29] F. Massines, P. Segur, N. Gherardi, C. Khamphan, A. Rocard, *Surf. Coating Technol.* **2003**, *174–175*, 8.
[30] R. H. Stark, K. H. Schoenbach, *Appl. Phys. Lett.* **1999**, *74*, 3770.
[31] K. H. Schoenbach, M. Moselhy, W. Shi, R. Bentley, *J. Vac. Sci. Technol., A* **2003**, *21*, 1260.
[32] L. Bardos, H. Barankova, *Surf. Coat. Technol.* **2000**, *133–134*, 522.
[33] J. G. Kang, H. S. Kim, S. W. Ahn, H. S. Uhm, *Surf. Coat. Technol.* **2003**, *144–148*, 171.
[34] J. Castro, M. H. Guerra-Mutis, H. J. Dulce, *Plasma Chem. Plasma Process.* **2003**, *23*, 297.
[35] K. H. Gericke, C. Geßner, P. Scheffler, *Vacuum* **2002**, *65*, 291.
[36] L. Baars-Hibbe, C. Schrader, P. Sichler, T. Cordes, K. Gericke, A. Büttgenbach, S. Draeger, *Vacuum* **2004**, *73*, 327.
[37] P. Sichler, A. Büttgenbach, L. Baars-Hibbe, C. Schrader, K. Gericke, *Chem. Eng. J.* **2004**, *101*, 465.
[38] J. H. Kim, Y. H. Kim, Y. H. Choi, W. Choe, J. J. Choi, Y. S. Hwang, *Surf. Coat. Technol.* **2003**, *144–148*, 171.
[39] I. E. Kieft, N. A. Dvinskikh, J. L. V. Broers, D. W. Slaaf, E. Stoffels, *Proc. SPIE* **2004**, *5483*, 247.
[40] K. Inomata, H. Ha, K. A. Chaudhary, H. Koinuma, *Appl. Phys. Lett.* **1994**, *64*, 46.
[41] H. Koinuma, H. Ohkubo, T. Hashimoto, K. Inomata, T. Shiraishi, A. Miyanaga, S. Hayashi, *Appl. Phys. Lett.* **1992**, *60*, 816.
[42] A. Rahman, A. P. Yalin, V. Surla, O. Stan, K. Hoshimiya, Z. Yu, E. Littlefied, G. J. Collins, *Plasma Sources Sci. Technol.* **2005**, *13*, 537.
[43] A. El-Dakrouri, J. Yan, M. C. Gupta, M. Laroussi, Y. Badr, *J. Phys. D*: *Appl. Phys.* **2002**, *35*, 109.
[44] T. Terajima, H. Koinuma, *Appl. Surf. Sci.* **2004**, *223*, 259.
[45] N. Gherardi, S. Martin, F. Massines, *J. Phys. D*: *Appl. Phys.* **2000**, *33*, 104.
[46] Y. Sawada, S. Ogawa, M. Kogomo, *J. Phys. D*: *Appl. Phys.* **1995**, *28*, 1661.
[47] L. J. Ward, W. C. E. Schofield, J. P. S. Badyal, A. J. Goodwin, P. J. Merlin, *Langmuir* **2003**, *19*, 2110.
[48] J. Salge, *Surf. Coat. Technol.* **1996**, *80*, 1.
[49] A. Sonnenfeld, T. M. Tun, L. Zajickova, K. V. Kozlov, H. E. Wagner, J. F. Behnke, R. Hippler., *Plasmas Polym.* **2001**, *6*, 237.
[50] K. Schmidt-Szalowski, Z. Rÿzanek-Boroch, J. Sentek, Z. Rymuza, Z. Kusznierewicz, M. Misiak, *Plasmas Polym.* **2000**, *5*, 173.
[51] N. McSporran, M. L. Hitchman, S. E. Alexandrov, S. H. Shamlian, S. Turnbull, F. Tuema, *J. Phys. IV* **2002**, *12*, 4.
[52] K. H. Schoenbach, R. Verhappen, T. Tessnow, F. E. Peterkin, W. W. Byszewski, *Appl. Phys. Lett.* **1996**, *68*, 13.
[53] K. H. Schoenbach, A. El-Habachi, W. Shi, M. Ciocca, *Plasma Sources Sci. Technol.* **1997**, *6*, 468.
[54] M. T. Ngo, K. H. Schoenbach, G. A. Gerdin, J. H. Lee, *IEEE Trans. Plasma Sci.* **1990**, *18*, 669.
[55] A. Melzer, R. Flohr, A. Piel, *Plasma Sources Sci. Technol.* **1995**, *4*, 424.
[56] H. Barankova, L. Bardos, *Appl. Phys. Lett.* **2000**, *76*, 285.
[57] M. Moselhy, I. Petzenhauser, K. Frank, K. H. Schoenbach, *J. Phys. D*: *Appl. Phys.* **2003**, *36*, 2922.
[58] Y. B. Guo, F. C. N. Hong, *Appl. Phys. Lett.* **2003**, *82*, 337.
[59] J. Y. Jeong, S. E. Babayan, V. J. Tu, I. Henins, J. Velarde, G. S. Selwyn, R. F. Hicks, *Plasma Sources Sci.Technol.* **1998**, *7*, 282.

 © 2005 WILEY-VCH Verlag GmbH & Co. KGaA, Weinheim

[60] J. Y. Jeong, J. Park, I. Henins, S. E. Babayan, V. J. Tu, G. S. Selwyn, G. Ding, R. F. Hicks, *J. Phys. Chem.* **2000**, *104*, 8027.
[61] V. J. Tu, J. Y. Jeong, A. Schütze, S. E. Babayan, G. S. Selwyn, G. Ding, R. F. Hicks, *J. Vac. Sci. Technol., A* **2000**, *18*, 2799.
[62] J. Park, I. Henins, H. W. Hermann, G. S. Selwyn, R. F. Hicks, *J. Appl. Phys.* **2001**, *89*, 20.
[63] J. Park, I. Henins, H. W. Hermann, G. S. Selwyn, *Phys. Plasmas* **2000**, *7*, 3141.
[64] S. E. Babayan, J. Y. Jeong, A. Schütze, V. J. Tu, M. Moravej, G. S. Selwyn, R. F. Hicks, *Plasma Sources Sci. Technol.* **2001**, *10*, 573.
[65] S. E. Babayan, G. Ding, R. F. Hicks, *Plasma Chem. Plasma Process.* **2001**, *21*, 505.
[66] G. R. Nowling, S. E. Babayan, V. Jankovic, R. F. Hicks, *Plasma Sources Sci. Technol.* **2002**, *11*, 97.
[67] S. E. Babayan, G. Ding, G. R. Nowling, X. Yang, R. F. Hicks, *Plasma Chem. Plasma Process.* **2002**, *22*, 255.
[68] M. Moravej, S. E. Babayan, G. R. Nowling, X. Yang, R. F. Hicks, *Plasma Sources Sci. Technol.* **2004**, *13*, 8.
[69] X. Yang, M. Moravej, S. E. Babayan, G. R. Nowling, R. F. Hicks, *J. Nucl. Mater.* **2004**, *323*, 134.
[70] X. Yang, S. E. Babayan, R. F. Hicks, *Plasma Sources Sci. Technol.* **2003**, *12*, 484.
[71] J. Y. Jeong, S. E. Babayan, A. Schuetze, V. J. Tu, J. Park, I. Henins, G. S. Selwyn, R. F. Hicks, *J. Vac. Sci. Technol., A* **1999**, *17*, 2581.
[72] G. R. Nowling, S. E. Babayan, M. Moravej, X. Yang, M. Yajima, W. Hoffman, R. F. Hicks, *Plasma Sources Sci. Technol.*, in press.■Update available?■
[73] A. Schütze, J. Y. Jeong, S. E. Babayan, J. Park, G. S. Selwyn, R. F. Hicks, *IEEE Trans. Plasma Sci.* **1998**, *26*, 1685.
[74] J. W. Nilsson, S. A. Riedel, *Electric Circuits*, Prentice-Hall, Englewood Cliffs, NJ **2000**.
[75] S. K. Ray, C. K. Maiti, S. K. Lahiri, N. B. Chakrabarti, *Adv. Mater. Opt. Electron.* **1996**, *6*, 73.
[76] S. P. Mukherjee, P. E. Evans, *Thin Solid Films, 1972, 14*, 105.
[77] Y. Qi, Z. G. Xiao, T. D. Mantei, *J. Vac. Sci. Technol., A* **2003**, *21*, 1064.
[78] W. J. Patrick, G. C. Schwartz, J. D. Chapple-Sokol, R. Carruthers, K. Olsen, *J. Electrochem. Soc.* **1992**, *139*, 2604.
[79] S. Sahli, S. Rebiai, P. Raynaud, Y. Segui, A. Zenasni, S. Mouissat, *Plasmas Polym.* **2002**, *7*, 327.
[80] Q. Wu, K. K. Gleason, *Plasma Polym.* **2003**, *8*, 31.
[81] J. A. Theil, D. V. Tsu, M. W. Watkins, S. S. Kim, G. Lucovsky, *J. Vac. Sci. Technol., A* **1990**, *8*, 1374.
[82] G. Lucovsky, P. D. Richard, D. V. Tsu, S. Y. Lin, R. J. Markunas, *J. Vac. Sci. Technol., A* **1986**, *4*, 681.■Journal name OK?■
[83] P. G. Pai, S. S. Chao, Y. Takagi, G. Lucovsky, *J. Vac. Sci. Technol., A* **1986**, *4*, 689.
[84] T. Matsutani, T. Asanuma, C. Liu, M. Kiuchi, T. Takeuchi, *Surf. Coat. Technol.* **2000**, *177–178*, 365.
[85] O. Zywitzki, H. Sahm, M. Krug, H. Morgner, M. Neumann, *Surf. Coat. Technol.* **2000**, *133–134*, 555.
[86] K. Teshima, Y. Inoue, H. Sugimura, O. Takai, *Thin Solid Films* **2002**, *420–421*, 324.
[87] J. S. Chou, S. C. Lee, *J. Appl. Phys.* **1995**, *77*, 1805.
[88] C. Doughty, D. C. Knick, J. B. Bailey, J. E. Spencer, *J. Vac. Sci. Technol., A* **1999**, *17*, 2612.
[89] S. Leclerc, A. Lecours, M. Carson, E. Richard, G. Turcotte, J. F. Currie, *J. Vac Sci. Technol.*, A **1998**, *16*, 881.
[90] D. Landheer, N. G. Skinner, T. E. Jackman, *J. Vac Sci Technol., A* **1991**, *9*, 2594.
[91] J. Yota, J. Handler, A. A. Saleh, *J. Vac. Sci. Technol., A* **2000**, *18*, 372.
[92] D. E. Kotecki, J. D. Chapple-Sokol, *J. Appl. Phys.* **1995**, *77*, 1284.
[93] S. Bae, D. G. Farber, S. J. Fonash, *Solid-State Electron.* **2000**, *44*, 1355.
[94] S. E. Alexandrov, M. L. Hitchman, S. Shamlian, *Adv. Mater. Opt. Electron.* **1993**, *2*, 301.
[95] J. A. Theil, S. V. Hattangady, G. Lucovsky, *J. Vac. Sci. Technol., A* **1992**, *10*, 719.
[96] D. L. Smith, A. S. Alimoda, F. J. von Presissig, *J. Vac. Sci. Technol., B* **1990**, *8*, 551.
[97] B. Anthony, T. Hsu, L. Breaux, R. Qian, S. Banerjee, A. Tasch, *J. Electron. Mater.* **1990**, *19*, 1089.
[98] S. W. Lee, D. C. Heo, J. K. Kang, Y. B. Park, S. W. Rhee, *J. Electrochem. Soc.* **1998**, *145*, 2900.
[99] W. M. M. Kessels, R. J. Severens, A. H. M. Smets, B. A. Korevaar, G. J. Adriaenssens, D. C. Schram, M. C. M. van de Sanden, *J. Appl. Phys.* **2001**, *89*, 2404.
[100] J. N. Lee, B. J. Lee, D. G. Moon, B. T. Ahn, *Jpn. J. Appl. Phys.*■Part 1 or Part 2? Also Ref 108?■ **1997**, *36*, 6862.
[101] L. S. Sidhu, S. Zukotynski, *J. Non-Cryst. Solids* **1999**, *246*, 65.
[102] R. J. Severens, G. J. H. Brussaard, M. C. M. van de Sanden, D. C. Schram, *Appl. Phys. Lett.* **1995**, *67*, 491.
[103] N. M. Johnson, J. Walker, C. M. Doland, K. Winer, R. A. Street, *Appl. Phys. Lett.* **1989**, *54*, 1872.
[104] G. Oversluizen, W. H. M. Lodders, *J. Appl. Phys.* **1998**, *83*, 8002.
[105] G. Lavareda, C. Nunes de Carvalho, A. Amaral, J. P. Conde, M. Vieira, V. Chu, *Vacuum* **2002**, *64*, 245.
[106] J. Qiao, Z. Jiang, Z. Ding, *J. Non-Cryst. Solids* **1985**, *77–78*, 829.
[107] K. Miyazaki, T. Kajiwara, K. Uchino, K. Muraoka, T. Okada, M. Maeda, *J. Vac. Sci. Technol., A*, **1997**, *15*, 149.
[108] K. Tachibana, *Jpn. J. Appl. Phys.* **1994**, *33*, 4329.
[109] S. Agarwal, S. Sriraman, A. Takano, M. C. M. van de Sanden, E. S. Aydil, D. Maroudas, *Surf. Sci.* **2002**, *515*, L469.
[110] S. P. Walch, S. Ramalingam, S. Sriraman, E. S. Aydil, D. Maroudas, *Chem. Phys. Lett.* **2001**, *344*, 249.
[111] W. Widdra, S. I. Yi, R. Maboudian, G. A. D. Briggs, W. H. Weinberg, *Phys. Rev. Lett.* **1995**, *74*, 2074.

© WILEY-VCH

Review: In this manuscript, a review is provided of atmospheric pressure PECVD of thin films using a capacitively coupled plasma source. The organometallic precursors are fed downstream of the plasma, where reactions occur exclusively between neutral molecules, radicals, and the substrate surface. As a result, the properties of the films are different than those obtained in low-pressure gas discharges (<1 torr).

M. Moravej, R. F. Hicks*

Chem. Vap. Deposition **2005**, *11*, 469 ... 476

Atmospheric Plasma Deposition of Coatings Using a Capacitive Discharge Source

 © 2005 WILEY-VCH Verlag GmbH & Co. KGaA, Weinheim